Misspecification under the Narrowband Assumption: A Cramér–Rao Bound Perspective

S. Semper*, E. Pérez′, M. Landmann†, R. Thomä*

***Abstract*—To efficiently extract estimates about the propagation behavior of electromagnetic waves in a radio environment it is common to invoke the narrowband-assumption. It essentially states that the relative bandwidth of the measurement system is so low that the frequency response of a single propagation path only depends on it Time-of-Flight and the response of the measurement device can be calibrated independently of the measured channel.**

Recent advances into higher relative bandwidths and antenna arrays with larger spatial aperture render this assumption less likely to be satisfied, which leads to a model mismatch during estimation. In this case estimates are inherently biased and have a special statistical behavior. This behavior can be captured by the so-called Misspecified Cramér-Rao Bound, which formulates a lower bound for the variance of estimates that are biased due to model mismatch.

We analyze this bound in contrast to the traditional Cramér-Rao Bound and show the shortcomings in the setting of joint ToF-DoA estimation in the mmWave spectrum. The conducted numerical studies also show that planar array geometries inherently suffer from violation of the narrowband assumption irrespective of the individual elements' frequency response, whereas circular structures show it to a lesser degree.

I. Introduction

Knowledge about the propagation behavior of radio channels is of importance in mobile communications, localization and sensing applications. To gain insights into the propagation, one conducts channel sounding measurements followed by post-processing to extract the quantities of interest [1]. These measurements are usually carried out in the spectral, temporal and spatial domains. For this task wideband channel sounders are used to measure an environment with wideband signals via arrays of antennas both at the transmitter (TX) and receiver (RX) site. To process these so-called multiple input multiple output (MIMO) snapshots, one formulates a suitable inverse problem that makes use of a parametric forward-model and estimates the parameters of interest [2].

One can derive such a model by making assumptions about the propagation behavior of the electromagnetic waves and the frequency response of the measurement device. We consider the specular ray model, which models the propagation via plane waves traveling from TX to RX. The parameters describing such a single plane wave are Time-of-Flight (ToF), Doppler-frequency, Direction of Departure (DoD) at TX, Direction of Arrival (DoA) at the RX and its polarization dependent attenuation and phase shift [3].

The influence of the measurement device that cannot be accounted for completely prior to processing of the data is the frequency-, polarization- and angle-dependent response of the used antenna elements. Since this response depends on the parameters of interest, i.e. DoD and DoA it has to be incorporated into the forward model upon estimation [4].

Once such a model is completely specified it is used to pose a specific inverse problem, for which one derives an algorithm to extract the propagation parameters from captured measurement data. Any solver of such an inverse problem that reaches a certain statistical quality when applied to noisy measurement data is called a High Resolution Parameter Estimator (HRPE). The performance of estimators can only be evaluated statistically, since the data is modeled as a realization of a random variable.

To assess the quality of such an estimator, one can evaluate its first and second order statistics, i.e. its bias and variance. An estimator that in expectation is able to recover the true parameters is called unbiased. For the class of unbiased estimators, those with minimum variance are of high interest, since they are considered optimal in this sense. Given assumptions about the distribution of the data, e.g. it being a Gaussian distribution, the so-called Cramér-Rao Bound (CRB) gives the minimum variance any unbiased estimator can achieve based on the mean and covariance of the data.

The CRB allows quantifying how suitable a specific measurement process is to extract the parameters of interest [5], and it determines the quality of estimation frameworks by serving as a theoretical and algorithm-independent benchmark [6]. Also, it allows describing how a scenario behaves in terms of the mean squared error (MSE) without the need for complex Monte-Carlo simulations involving estimation routines.

For that it is necessary that the considered estimators are unbiased. One necessary condition for unbiasedness is that the parametric model correctly captures the behavior of the measurement data, i.e. it is correctly specified. In our considered problem of channel estimation one usually employs the so-called narrowband assumption [2], [7]. Although we are generating, capturing and processing data occupying an extended bandwidth, due to the small relative bandwidth we assume that only the ToF of a single plane wave is influencing the frequency response and that the scattering within the environment and the responses of the antennas are constant enough over the measured frequency band. However, the physical processes are frequency-dependent [8], [9] such that every captured data sample does only approximately satisfy this assumption.

* Technische Universität Ilmenau, EMS, Ilmenau, Germany, † Fraunhofer IIS, Department EMS Ilmenau, Germany, ′ Fraunhofer Institute for Nondestructive Testing IZFP, Saarbrücken, Germany; This work is partly funded by the DFG projects HoPaDyn with Grant-No. TH 494/30-1 and JCRS-CoMP with Grant-No. TH 494/35-1 and Fraunhofer Internal Programs under the grant Attract 025-601128

The driving motivations to make this assumption are a lower computational complexity [2] during the estimation and lower calibration efforts for the measurement device prior and during estimation [10].

Ultimately, this assumption results in a so-called misspecified parametric model, which generally yields an inherently biased estimator, for which the CRB is not applicable. Still, many performance analyses are carried out as if the narrowband assumption holds in practice and comparisons of algorithms are made based on this. If however, the algorithms' comparisons do not factor in the violation of the narrowband assumption into the analysis, the theoretical findings that rely on the CRB have only very limited carry over to real world scenarios, where it is never satisfied. In other cases, the CRB is used as a reference during the execution of an estimation algorithm itself to determine the validity of the current estimate [2]. We show that neglecting this phenomenon, can have a drastic influence on the conclusions drawn based on the CRB, since in some cases it differs significantly from the Misspecified Cramér-Rao Bound (MCRB). Fortunately, in recent years the analysis of estimators resulting from misspecified models has gained much attention, resulting in the MCRB as a natural extension of the CRB in this more general setting. As such, it allows to still make statements about the statistical performance of the least biased estimators under this model mismatch, again given in some suitable second-order statistics.

We want to first shortly introduce the theory related to the MCRB and then put it in the context of channel estimation and the narrowband assumption. The aim is to start a discussion in the field of HRPE, especially when moving to the mmWave spectrum and beyond, where higher relative bandwidths are considered for channel sounding. We use numerical experiments to shed light on some effects that one encounters when moving from the CRB to the MCRB, and we use the discrepancy between the MCRB and the CRB as a proxy to determine to what degree the narrowband assumption is violated. The findings from these explorative studies can be summarized as follows:

- As intuitively expected, the discrepancy between the CRB and the MCRB increases for larger relative bandwidths.
- When we employ a planar array geometry for the spatial measurements, the discrepancy between CRB and MCRB increases also for fixed bandwidth and fixed array element spacing but larger aperture, i.e. more elements in the array.
- In contrast to the planar array structure, a stacked circular structure (cylindrical) shows this discrepancy to a lesser degree, i.e. less discrepancy between CRB and MCRB.

To commence, we first need a short recap of the theoretical basics about estimators and their statistical behavior.

II. Lower Bounds for Misspecified Estimators

Let a full MIMO observation $\boldsymbol{y} \in \mathbb{C}^N$ follow a distribution G with density f_G and let us use a parametric model $\mathcal{F} : \Theta \to \{F | F : \Omega \to \mathbb{C}^N\}$ with $\Theta \subset \mathbb{R}^T$ such that for every $\boldsymbol{\theta} \in \Theta$ we get a distribution $\mathcal{F}(\boldsymbol{\theta})$ with probability density function (pdf) $f(\cdot|\boldsymbol{\theta}) : \mathbb{C}^N \to [0, 1]$.

In our specific case of channel estimation Θ contains all possible parameters to model a MIMO snapshot in a multipath scenario using the narrowband assumption and the specular ray model. Due to the misspecification, there is no $\boldsymbol{\theta} \in \Theta$ such that $G = \mathcal{F}(\boldsymbol{\theta})$.

The best we can hope for is to find a $\boldsymbol{\theta}$ such that the Kullback-Leibler Divergence (KLD) $D(f_g \| f(\cdot|\boldsymbol{\theta}))$ defined as

$$D(f_1 \| f_2) = \int\limits_{\mathbb{C}^N} \ln\left(\frac{f_1(\boldsymbol{x})}{f_2(\boldsymbol{x})}\right) \cdot f_1(\boldsymbol{x}) \, \mathrm{d}\boldsymbol{x} \quad (1)$$

is minimal with respect to $\boldsymbol{\theta}$. If there is a unique $\boldsymbol{\theta}^*$ minimizing D, then $\boldsymbol{\theta}^*$ is called the Pseudo-True Solution (PTS). Any estimator $\hat{\boldsymbol{\theta}}$ that satisfies $\mathbf{E}(\hat{\boldsymbol{\theta}}(\boldsymbol{y})) = \boldsymbol{\theta}^*$ is called misspecified-unbiased (MS-unbiased), since in expectation it is able to recover $\boldsymbol{\theta}^*$ from data $\boldsymbol{y}$.

Based on $f(\cdot|\boldsymbol{\theta})$ and data $\boldsymbol{y}$ we can define the misspecified log-likelihood $\lambda : \Theta \to \mathbb{R}_0^+$ via

$$\lambda(\boldsymbol{\theta}) = \ln f(\boldsymbol{y}|\boldsymbol{\theta}) \quad (2)$$

and two matrices $\boldsymbol{A}, \boldsymbol{B} \in \mathbb{R}^{T \times T}$

$$A_{i,j} = \mathbf{E}\left[\frac{\partial \lambda(\boldsymbol{\theta}^*)}{\partial \theta_i \partial \theta_j}\right], B_{i,j} = \mathbf{E}\left[\left(\frac{\partial \lambda(\boldsymbol{\theta}^*)}{\partial \theta_i}\right)\left(\frac{\partial \lambda(\boldsymbol{\theta}^*)}{\partial \theta_j}\right)\right]. \quad (3)$$

Last, define the error covariance $\boldsymbol{C} : \Theta \to \mathbb{R}^{T \times T}$ depending on the PTS $\boldsymbol{\theta}^*$ as

$$C_{i,j}(\boldsymbol{\theta}) = \mathbf{E}\left[(\theta_i - \theta_i^*)(\theta_j - \theta_j^*)\right] \quad (4)$$

If the matrix $\boldsymbol{A}$ is invertible and the estimator $\hat{\boldsymbol{\theta}}$ is MS-unbiased, the *Misspecified Cramér-Rao Bound* states that the errors' covariance $\boldsymbol{C}$ satisfies

$$\boldsymbol{C}(\hat{\boldsymbol{\theta}}) \succeq \boldsymbol{A}^{-1}\boldsymbol{B}\boldsymbol{A}^{-1}, \quad (5)$$

which means $\boldsymbol{C}(\hat{\boldsymbol{\theta}}) - \boldsymbol{A}^{-1}\boldsymbol{B}\boldsymbol{A}^{-1}$ is positive semi-definite. Usually one is interested in the so-called misspecified mean squared error (MMSE), i.e. the diagonal entries of $\boldsymbol{C}$, namely

$$C_{i,i}(\boldsymbol{\theta}) = \mathbf{E}\left[(\theta_i - \theta_i^*)^2\right].$$

Note that in the correctly specified case, an MS-unbiased estimator $\hat{\boldsymbol{\theta}}$ is naturally unbiased, and we have that $-\boldsymbol{A} = \boldsymbol{B}$, such that (5) recovers the conventional CRB and $\boldsymbol{C}$ is a lower bound for the MSE.

In this publication, we assume that the only source for misspecification is the oversimplified model of the antenna response. Hence, it is valid to model both G and $\mathcal{F}(\boldsymbol{\theta})$ as complex Gaussian distributions with equal covariance $\boldsymbol{\Sigma} \in \mathbb{C}^{N \times N}$ but different means. Then, our misspecified parametric model for $\boldsymbol{y} \sim \mathcal{N}(\boldsymbol{\mu}, \boldsymbol{\Sigma})$ is defined by a function $\boldsymbol{s} : \Theta \to \mathbb{C}^N$ and results in $\mathcal{F}(\boldsymbol{\theta}) = \mathcal{N}(\boldsymbol{s}(\boldsymbol{\theta}), \boldsymbol{\Sigma})$, where $\boldsymbol{s}(\boldsymbol{\theta}) \neq \boldsymbol{\mu}$ for all $\boldsymbol{\theta} \in \Theta$. Under the assumption of Gaussian distributions and smooth $\boldsymbol{s}$ the matrices $\boldsymbol{A}$ and $\boldsymbol{B}$ can be computed in closed form.

The only quantity still elusive is the PTS, since it is not clear how to minimize D or how to prove we have minimized D. Luckily, given some suitable regularity conditions, the estimator

$$\hat{\boldsymbol{\theta}} = \underset{\boldsymbol{\theta} \in \Theta}{\operatorname{argmax}} \, \lambda(\boldsymbol{\theta}), \quad (6)$$

called the Misspecified Maximum-Likelihood Estimator (MMLE), is asymptotically MS-unbiased and (5) is an equality in this case. In our case, we are going to use RIMAX [2] as the ML estimator, to obtain the PTS.

III. Explorative Numerical Analysis

Since the scenarios we are going to study are too complex for closed form expressions either for the CRB or the MCRB, we will carry out the evaluations purely based on numerical versions of (5), but with analytic expressions for $\boldsymbol{A}$ and $\boldsymbol{B}$. In our case of Gaussian distributions, there are formulas [11] reminiscent of the Slepian–Bangs formula [12] for the Fisher Information Matrix (FIM) in case of Gaussian likelihood estimation.

The scenario we are going to study is a static, broadband Single Input Multiple Output (SIMO) setting, where we employ a single perfectly isotropic antenna at TX and an antenna array at RX where we take equi-spaced measurements in frequency domain from f_0 to f_1. We collect these frequencies in a vector $\boldsymbol{\phi} \in \mathbb{R}^{N_f}$. Further, assume that the measurement system has been fully calibrated offline, such that the only part of the measurement system that has to be accounted for are the N_r different polarization-, angle- and frequency-dependent antenna beampatterns at RX. The parameters we estimate are ToF and DoA. With respect to these all errors and bounds are calculated. Finally, these beampatterns will also be our only source of model-mismatch in the sense that we assume these to be frequency independent, when in reality they are not.

The true model we use to generate the data is $\boldsymbol{s}^{\mathrm{t}} : \Theta \to \mathbb{C}^{N_f \times N_r}$ and it reads as

$$\boldsymbol{s}^{\mathrm{t}}_{f,r}(\boldsymbol{\theta}) = \sum_{p=1}^{P} \boldsymbol{\gamma}_{e,p} \cdot \boldsymbol{a}^{\mathrm{rx}}_{f,r,e}(\vartheta_p, \varphi_p) \cdot \exp(\jmath 2\pi \boldsymbol{\phi}_f \tau_p), \quad (7)$$

where $\gamma_{e,p} \in \mathbb{C}^2$, $\vartheta_p \in [0, \pi]$, $\varphi_p \in [-\pi, +\pi]$ and $\tau_p \in [0, 1]$ denote the polarimetric pathweight, co-elevation and azimuth and ToF of the p-th propagation path impinging at RX respectively. This renders the parameter space $\Theta \in \mathbb{R}^{P \cdot 7}$. The key component here is that the function $\boldsymbol{a}^{\mathrm{rx}}_{f,r,e}$ represents the farfield beampattern of the r-th antenna element at frequency $\boldsymbol{\phi}_f$ for electric field component e, which models the response to one of two orthogonal excitation modes (usually denoted H and V) [13]. Note that this directly shows that $\boldsymbol{s}^{\mathrm{t}}$ is *not* invoking the narrowband assumption, since it accounts for a changing antenna response over frequency.

The model $\boldsymbol{s} : \Theta \to \mathbb{C}^{N_f \times N_r}$ using this assumption then naturally reads as

$$\boldsymbol{s}_{f,r}(\boldsymbol{\theta}) = \sum_{p=1}^{P} \boldsymbol{\gamma}_{e,p} \cdot \boldsymbol{a}^{\mathrm{rx}}_{r,e}(\vartheta_p, \varphi_p) \cdot \exp(\jmath 2\pi \boldsymbol{\phi}_f \tau_p), \quad (8)$$

where the interpretation of the parameters in comparison to (7) has not changed. Henceforward, each data sample we consider is going to be of the form

$$\boldsymbol{y} = \boldsymbol{s}^{\mathrm{t}}(\boldsymbol{\theta}_0) + \boldsymbol{n}^{\mathrm{t}} \quad (9)$$

for some white Gaussian complex circularly symmetric noise-vector $\boldsymbol{n}^{\mathrm{t}} \sim \mathcal{N}(\boldsymbol{0}, \sigma^2 \boldsymbol{I}_{N_f \times N_r})$, where $\boldsymbol{I}_{N_f \times N_r}$ is the identity matrix. However, we are going to *assume* it is of the form

$$\boldsymbol{y} = \boldsymbol{s}(\boldsymbol{\theta}_0) + \boldsymbol{n}, \quad (10)$$

which introduces the misspecification. Here, $\boldsymbol{n}$ is assumed to follow the same distribution as $\boldsymbol{n}^{\mathrm{t}}$. We will compare the estimation bounds in the sense that we use $\boldsymbol{s}^{\mathrm{t}}$ to generate the true data and estimate it with the model $\boldsymbol{s}$. In our specific case we use a frequency dependent description of the antenna response to calculate $\boldsymbol{s}^{\mathrm{t}}$, while we use the respective single-frequency beampattern at the considered center frequency in $\boldsymbol{\phi}_f$ to evaluate $\boldsymbol{s}$.

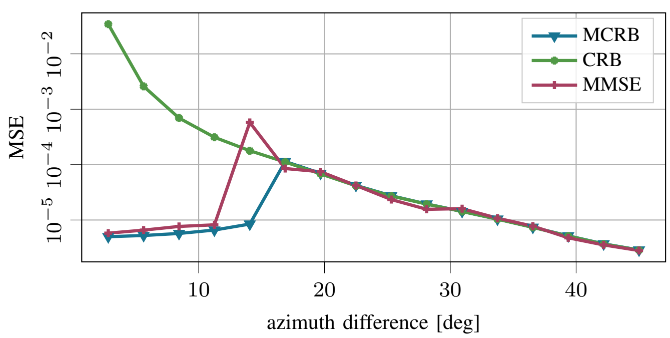

Fig. 1. *The MMSE agrees with the MCRB* – MMSE and bounds for a 2-path scenario at 3 GHz bandwidth around 26.5 GHz and a 3×8 StUCA depending on the sources' distance in azimuth.

Also, in any case we use Monte-Carlo simulations over multiple noise realizations and calculate $\|\boldsymbol{\theta}^* - \hat{\boldsymbol{\theta}}\|_2^2$ from an estimate $\hat{\boldsymbol{\theta}}$ to get estimates of the MMSE in a certain parameter constellation. The PTS $\boldsymbol{\theta}^*$ is computed using RIMAX where we assume knowledge of the correct number of sources and the noise variance. For the CRB computations, we evaluate (5) for the case $\boldsymbol{A} = -\boldsymbol{B}$ at the true but unknown parameter $\boldsymbol{\theta}_0$ in (7), as it is usually done in practice. For the MCRB we evaluate (5) at the retrieved PTS. Unless stated otherwise we use a fixed Signal-to-Noise Ratio (SNR) of 20 dB. Additionally, no matter the bandwidth, we choose $\Delta f = 50\,\mathrm{MHz}$ as sampling distance in frequency domain.

A. Synthetic Stacked Uniform Circular Array

Let us first consider an array geometry of ideal (read: synthetic) Hertzian dipoles. At each spatial sampling location, we place a pair of two dipoles oriented such that they are sensitive to orthogonal polarizations. The physical length of the dipole corresponds to the wavelength at the center of the used frequency band. We use these "polarimetric" dipoles as single elements in a stacked circular array structure consisting of 3 rings containing 8 elements each, which is a popular geometry employed in channel sounding. To avoid spatial aliasing we choose the spacing of the elements that they obey the $\lambda/2$-criterion both across the rings and within the rings. We use the readily available closed form solutions for the frequency-dependent farfield beampattern of a Hertzian dipole as found in [14, p. 133–151].

We consider a two-source scenario, where one source is kept fixed at delay $\tau_1 = 0.5$, co-elevation $\vartheta_1 = \pi/2$ and azimuth $\varphi_1 = 0$. For the second source we choose the same parameters and only vary φ_2. The results are depicted in Figure 1, which we obtained for a bandwidth from 25 GHz to 28 GHz. For larger $|\varphi_1 - \varphi_2|$ all three quantities agree very well, whereas for smaller distance between the two paths – practically the more interesting case – we see a stark deviation of the CRB from the MCRB. More importantly the latter is able to predict the behavior of the MMSE correctly. This simple scenario already shows a shortcoming in prediction accuracy of the CRB. It is also noteworthy that the relative bandwidth of 4 %

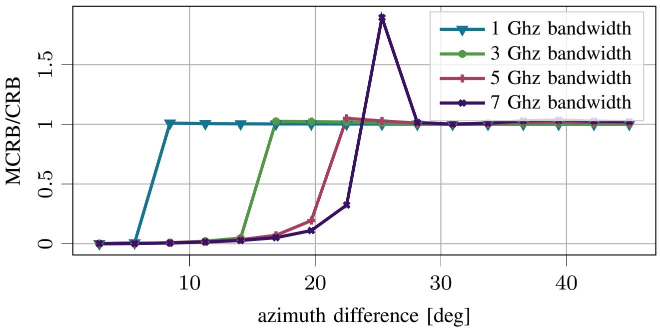

Fig. 2. *The area of stark deviation of the CRB from the MCRB increases for larger relative bandwidths* – Ratio of the bounds for different bandwidths for a 2-path scenario and a 3×8 StUCA depending on the sources' distance in azimuth.

is usually not considered large enough motivating us to drop the narrowband-assumption.

We now repeat above simulations for different bandwidths, where the lower frequency is fixed at 25 GHz. Figure 2 depicts the ratio of the calculated estimation bounds, where values far from 1 indicate a large deviation of the CRB from the MCRB and values closer the opposite. As expected, the difference between the two bounds increases with increasing relative bandwidth in the sense that the azimuth interval where the two bounds disagree is increasing. What is also astonishing is the fact that the CRB predicts a higher MSE than the results yield. This is due to the fact that the CRB is evaluated at the true $\boldsymbol{\theta}_0$ whereas the MCRB is evaluated at the PTS $\boldsymbol{\theta}^*$. Not only are different expressions evaluated, but also at possibly different locations. The fact that the MCRB is lower than the CRB does not mean that the estimate from the misspecified model is “more accurate” than predicted by the CRB.

B. Synthetic Aperture Uniform Rectangular Array

For the above simulations we employed a entirely synthetic antenna model based on a dipole. Now we aim at incorporating measured beampatterns into our calculations. To this end, we use the antenna data of the Synthetic Aperture Measurements of Uncertainty in Angle of Incidence (SAMURAI) measurement system[15] developed at National Institute of Standards and Technology (NIST)[1]. The system consists of a single open-ended waveguide that is moved by a robotic arm to acquire spatial samples, thus forming a synthetic aperture. The main feature of this antenna is that it behaves very stable across the considered bandwidths both in amplitude and phase. As such its response can be approximated well by the beampattern of the respective center frequency. Hence, there is no indication for a severe violation of the narrowband assumption.

In our experiments we are going to consider a Uniform Rectangular Array (URA) structure with $n_{\mathrm{rx}} \times n_{\mathrm{rx}}$ many elements obeying the spatial sampling theorem at the respective upper frequency considered. The lower frequency is kept fixed at 27 GHz and the upper frequency limit is adjusted accordingly.

We consider a scenario with 6 GHz of bandwidth, a 17×17 URA structure oriented perpendicular to the spherical basis

[1]We thank Damla Guven and Camillo Gentile for providing the data and NIST for the permission to use it.

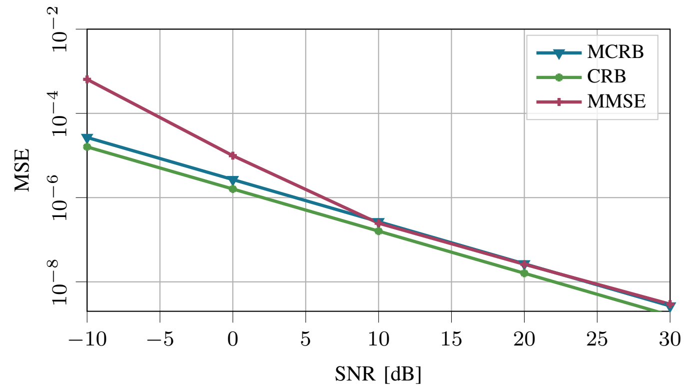

Fig. 3. *The MMSE agrees with the MCRB* – MMSE and bounds for a 2-path scenario at 6 GHz bandwidth (5 % relative bandwidth at 30 GHz) and a 17×17 URA depending on the SNR.

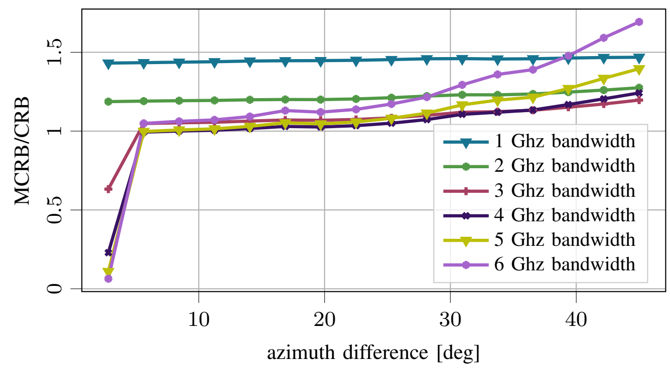

Fig. 4. *Increasing the bandwidth increases the misspecification due to the narrowband assumption* – Ratio of the bounds for different bandwidths for a 2-path scenario and a 17×17 URA depending on the sources' distance in azimuth.

vector $\boldsymbol{e}_r$ at co-elevation $\pi/2$, azimuth 0 and radial part 1. We simulate a two-source scenario, where one source is kept fixed at delay $\tau_1 = 0.5$, co-elevation $\vartheta_1 = \pi/2$ and azimuth $\varphi_1 = 0$. For the second source we choose the same parameters as for the first source and set $\varphi_2 = \pi/(2 \cdot 17)$. In Figure 3 the MMSE perfectly aligns with the MCRB once the estimation algorithm is in the SNR regime where it is producing valid solutions. However, one can also see that both the CRB and MCRB scale linearly with the SNR on a logarithmic scale as expected.

We stay with this two-source scenario and the 17×17 URA structure as above, where for the second source we choose the same parameters as for the first and only vary φ_2. Figure 4 shows that the disagreement between CRB and MCRB increases proportionally with the increase in bandwidth. For closely spaced sources, a similar behavior as in Figure 2 is visible that the disagreement between the bounds rapidly increases. Also, compare this to Figure 2, where the disagreement between the MCRB and the CRB only happens for low angular difference of the two sources but not for large ones as in Figure 4.

What is usually done to improve the angular resolution is to increase the number of antenna elements. The beamwidth of such an array is steadily decreasing for more elements, i.e. a larger spatial aperture. The farfield and frequency-dependent steering vector of this array can be expressed as

$$\boldsymbol{a}_{f,e}(\vartheta, \varphi) = \boldsymbol{a}^{\mathrm{wg}}_{f_c}(\vartheta, \varphi) \cdot \exp(\jmath 2\pi \cdot \boldsymbol{\phi}_f \cdot \langle \boldsymbol{p}_e, \boldsymbol{r}(\vartheta, \varphi) \rangle), \quad (11)$$

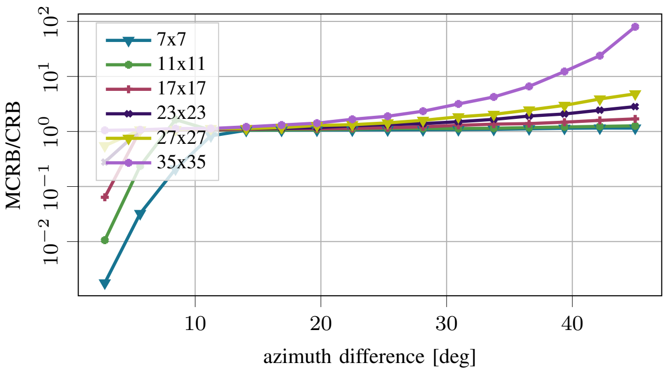

Fig. 5. *Increasing the spatial aperture increases the misspecification due to the narrowband assumption* – Ratio of the bounds for different aperture sizes of the URA for a 2-path scenario at 6 GHz depending on the sources' distance in azimuth.

where $\boldsymbol{r}(\vartheta, \varphi) \in \mathbb{R}^3$ is the Cartesian coordinate where a ray from direction (ϑ, φ) pierces the unit sphere of $\mathbb{R}^3$ and $\boldsymbol{p}_e \in \mathbb{R}^3$ denotes the measurement position of the e-th element in the synthetic aperture. If we employ the narrowband-assumption at center frequency f_c, we calculate

$$\boldsymbol{a}_e(\vartheta, \varphi) = \boldsymbol{a}_{f_c}^{\mathrm{wg}}(\vartheta, \varphi) \cdot \exp(\jmath 2\pi \cdot f_c \cdot \langle \boldsymbol{p}_e, \boldsymbol{r}(\vartheta, \varphi) \rangle). \quad (12)$$

However, taking a close look at the expression unveils that for spatially larger apertures some elements have such a large $\|\boldsymbol{p}_e\|$ such that $\langle \boldsymbol{p}_e, \boldsymbol{r}(\vartheta, \varphi) \rangle$ extends over a considerable number of wavelengths resulting in a phase error when using $\boldsymbol{a}_e$ instead of $\boldsymbol{a}_{f,e}$ for those elements that are at the border of the URA and those frequencies at the edge of the considered band.

We expect for fixed bandwidth and increasing spatial size of the URA, the CRB and the MCRB must disagree more. This is reflected in Figure 5, where we repeated the simulations of Figure 4 for fixed bandwidth of 6 GHz but instead increasing the number of antenna elements in the URA. As can be inferred from the ratio of the bounds, the number of elements, i.e. the spatial dimension of the array, additionally contributes to the violation of the narrowband-assumption. As obvious from (11) and (12), this would also happen for a perfectly frequency-flat antenna response, since the effect results from the spatial distribution of the elements and this processes' frequency response, i.e. the resulting phase change over frequency.

IV. Conclusion

The numerical studies suggest that the employed RIMAX estimator is MS-unbiased, at least in the scenarios considered, since it can serve as a tool to obtain the PTS and also the resulting MMSE from its estimates follows the MCRB.

We use the discrepancy between the CRB and the MCRB as a proxy to infer how much the narrowband-assumption is violated. The simulations suggest that circular array structures suffer less severely from the use of higher bandwidths since the discrepancy between CRB and MCRB behaves more stable. Most surprisingly the results in Figure 5 suggest that for fixed bandwidth, the increase of the spatial aperture leads to a stark violation of the narrowband-assumption.

Concluding, we would like to point out that the MCRB is no measure for the *true* bias of the resulting estimates. The MCRB is a bound for the estimates' deviation from the PTS, which generally is biased away from the true parameter given model mismatch. From a practical point this bias of the PTS would be most interesting, but up until now it remains elusive in terms of theoretical bounds.

References

[1] H. Krim and M. Viberg, "Two decades of array signal processing research: The parametric approach," *IEEE Signal Process Mag.*, no. 4, 1996. DOI: 10.1109/79.526899.

[2] M. Haardt, R. Thomä, and A. Richter, "Multidimensional high-resolution parameter estimation with applications to channel sounding," English, in *High-Resolution and Robust Signal Processing*, Y. Hua, Ed. 2003.

[3] M. Steinbauer, A. Molisch, and E. Bonek, "The double-directional radio channel," *IEEE Antennas Propag. Mag.*, no. 4, 2001. DOI: 10.1109/74.951559.

[4] S. Semper, M. Döbereiner, C. Steinmetz, M. Landmann, and R. Thomä, "High Resolution Parameter Estimation for Wideband Radio Channel Sounding," 2023. DOI: 10.36227/techrxiv.22059656.v1.

[5] S. Pawar, S. Semper, and F. Romer, "Combining matrix design for 2D DoA estimation with compressive antenna arrays using stochastic gradient descent," in *ICASSP 2019 - 2019 IEEE International Conference on Acoustics, Speech and Signal Processing (ICASSP)*, IEEE, 2019. DOI: 10.1109/icassp.2019.8683173.

[6] F. Roemer, M. Ibrahim, N. Franke, N. Hadaschik, A. Eidloth, B. Sackenreuter, and G. Del Galdo, "Measurement matrix design for compressed sensing based time delay estimation," in *2016 24th European Signal Processing Conference (EUSIPCO)*, IEEE, 2016. DOI: 10.1109/eusipco.2016.7760290.

[7] J. Salmi and A. F. Molisch, "Propagation parameter estimation, modeling and measurements for ultrawideband MIMO radar," *IEEE Trans. Antennas Propag.*, no. 11, 2011. DOI: 10.1109/tap.2011.2164214.

[8] P. Barnes and F. Tesche, "On the direct calculation of a transient plane wave reflected from a finitely conducting half space," *IEEE Trans. Electromagn. Compat.*, no. 2, 1991. DOI: 10.1109/15.78345.

[9] A. Molisch, "Ultrawideband propagation channels-theory, measurement, and modeling," *IEEE Trans. Veh. Technol.*, no. 5, 2005. DOI: 10.1109/tvt.2005.856194.

[10] M. Landmann, M. Kaske, and R. S. Thoma, "Impact of incomplete and inaccurate data models on high resolution parameter estimation in multidimensional channel sounding," *IEEE Trans. Antennas Propag.*, no. 2, 2012. DOI: 10.1109/tap.2011.2173446.

[11] C. D. Richmond and L. L. Horowitz, "Parameter bounds under misspecified models," in *2013 Asilomar Conference on Signals, Systems and Computers*, 2013. DOI: 10.1109/ACSSC.2013.6810254.

[12] P. Stoica, R. L. Moses, *et al.*, *Spectral analysis of signals*. Pearson Prentice Hall Upper Saddle River, NJ, 2005.

[13] M. Landmann and G. D. Galdo, "Efficient antenna description for MIMO channel modelling and estimation," in *7th European Conference on Wireless Technology, 2004.*, 2004.

[14] C. A. Balanis, *Antenna Theory, Analysis and Design*. John Wiley & Sons, Inc., 2005.

[15] D. Guven, B. F. Jamroz, J. Chuang, C. Gentile, R. D. Horansky, K. A. Remley, D. F. Williams, J. T. Quimby, A. J. Weiss, and R. Leonhardt, "Methodology for measuring the frequency dependence of multipath channels across the millimeter-wave spectrum," *IEEE Open Journal of Antennas and Propagation*, 2022. DOI: 10.1109/OJAP.2022.3168401.